On the Measurement of the Grounding Impedance of Tall Wind Turbines

Alexander Smorgonskiy, Daniel Gazzana, Nicolas Mora, Marcos Rubinstein, Farhad Rachidi

Abstract—**In this work, we investigate experimentally the influence of the presence of tall wind turbines on the measured grounding impedance at their base. Two scenarios were considered: In the first one, measurements were carried out on the grounding system embedded in the wind turbine foundation, before assembly of the wind turbine itself; in the second one, the complete wind turbine (tower, nacelle and blades) was included. The frequency dependence of the grounding impedance was evaluated. A numerical simulation in steady state was also performed. The simulation model leads to a satisfactory representation of the studied system. Preliminary results show that the evaluated grounding impedance is affected by the presence of the complete wind turbine, especially at higher frequencies.**

Keywords: **Grounding impedance,** *in situ* **measurements, numerical simulation, wind turbine.**

I. INTRODUCTION

Grounding systems are essential for dissipating the current originating from a lightning discharge to the earth, functioning as an important component for protection and safety. Grounding systems present significant relevance, particularly in transmission networks and in the protection of devices subjected to high risk of failure caused by lightning strikes, as is the case of wind turbines (WT).

The use of renewable energy is a global trend and the development of the associated new technologies is a must. The reliability of wind parks in the mountains is of great concern because of their remote location, which significantly increases maintenance costs. In addition, wind turbines in the mountains have a high risk of failures due to lightning strikes [1]. Research on lightning protection of wind turbines is mainly focused on the protection of the blades, whereas proper grounding also plays an important role in the performance of the WT and its equipment during a lightning strike [2]-[5].

In this context, the goal of this paper is to present the results of wind turbine grounding impedance measurements performed at the Mont-Crosin wind park in Switzerland. Experiments were carried out (1) when only the construction of the wind turbine foundation had been completed, and (2) once the installation of the rest of the wind turbine was finished, namely the tower, nacelle and blades. In addition, numerical simulations to evaluate the performance of the grounding static resistance are presented.

II. WIND TURBINE PARK OVERVIEW

The Mont-Crosin wind park is located in the Jura Mountains and is composed of 16 WT with nominal power ranging from 850 kW to 2 MW, installed capacity of 29.2 MW and annual energy production above 40 GWh. Fig. 1 shows an aerial view of the wind park.

Fig. 1. Mont-Crosin wind park.

Even considering that the Mont-Crosin is not located in an area of high keraunic level[1], in the past years, a number of lightning flashes have hit several wind turbines, causing severe damage. Recently, during the repowering process, four new 2 MW units replaced the old ones (WT5, WT6, WT7 and WT8) and the opportunity was taken to begin a study on the behavior of the grounding system. The tower height of the referred WTs is 95 m, with a base diameter of 7.5 m, a rotor diameter of 90 m and total height of 140 m.

The grounding of the new wind turbines consists of a copper wire ring of 18 m diameter in its base, interconnected with several circular copper and aluminum conductors at different depths (6 m diameter for the top ring), linked to steel reinforced bars. This structure, also called concentrated

A. Smorgonskiy, D. Gazzana, N. Mora, F. Rachidi are with EMC Lab, Swiss Federal Institute of Technology EPFL, Lausanne, VD, 1015, Switzerland (e-mail: alexander.smorgonskiy@epfl.ch, daniel.dasilvagazzana@epfl.ch, nicolas.mora@epfl.ch, farhad.rachidi@epfl.ch).

D. Gazzana is with Department of Automation and Energy, UFRGS University, Porto Alegre, RS, 90035-190, Brazil (e-mail of corresponding author: daniel.dasilvagazzana@epfl.ch, dgazzana@ece.yfrgs.br).

M. Rubinstein is with University of Applied Sciences Western Switzerland, Yverdon-les-Bains, Switzerland (e-mail: marcos.rubinstein@heig-vd.ch).

---

[1] The ground flash density in the area is about 2-3 flashes per km^2 per year.

grounding, is filled with concrete and is encased in the tower foundation.

III. GROUNDING SYSTEM MEASUREMENTS

In 2016, several grounding transient measurements were carried out in the four new units. For space reasons, the study presented here will focus on only one of the wind turbines, WT6. In the experiments, different surge wave shapes were injected in the grounding system considering two scenarios: In the first one, the measurements were performed only on the grounding system embedded in the WT foundation (left panel in Figure 2); the second one took into account the complete WT, including the tower, the nacelle and the blades (right panel in Figure 2).

Fig. 2. Scenarios considered in the measurements: grounding system embedded in WT foundation (left panel); complete WT with tower, nacelle and blades (right panel).

A. Experiment setup

In the measurements, a surge impulse generator (Haefely RSG 482), an oscilloscope with 4 channels (LeCroy LT264 series), a current probe (Pearson 2877) and a passive voltage probe (Tektronix P5100) were used to perform the tests in both scenarios. Fig. 3 illustrates the measuring circuit and the related devices.
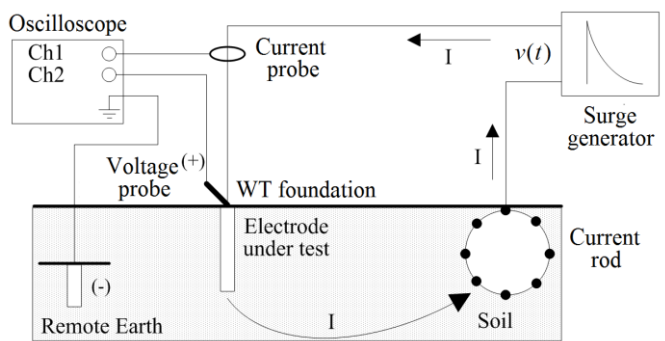

Fig. 3. Measuring circuit used in the experiments (Figure adapted from [6]).

Additionally, copper cables of 100 m length and 6 mm^2 cross-sectional area were used to connect the impulse generator to the current rod (underground current path) and the oscilloscope to the voltage rod (representing the remote earth).

B. Soil resistivity measurement

In order to determine the soil resistivity, measurements using the Wenner Method were performed in accordance with [7]-[8]. Four rods in alignment were embedded in the soil at a depth $l = 30$ cm and spaced apart by a distance $s = 1, 2, 3, 4, 6, 10, 30$ and 50 m.

The following characteristics were obtained: resistivity of the first layer $\rho_1 = 345.35$ Ωm; resistivity of the second layer $\rho_2 = 180.13$ Ωm and depth of the first layer $h = 0.77$ m.

C. Measurements considering only the foundation

Taking into account the circuit presented in Fig. 3, a voltage impulse represented by a double exponential shape was injected into the foundation of the wind turbine. Fig. 4 shows the measured voltage and current in this experiment.
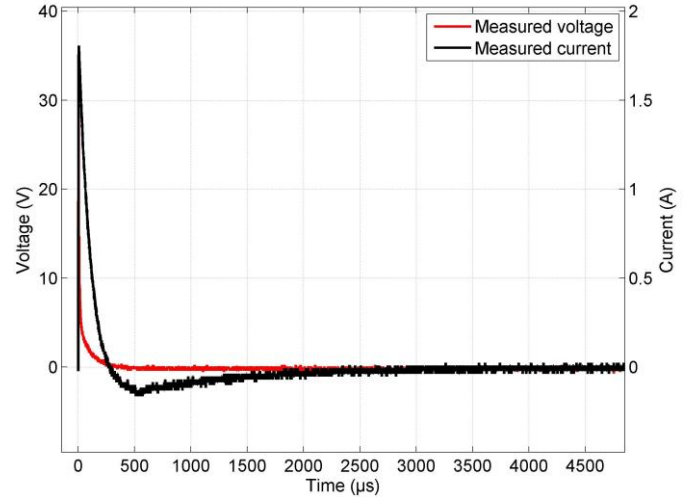

Fig. 4. Measured voltage and current injected into the wind turbine foundation (foundation only).

The adopted sampling rate was 20 MHz. Fig. 5 presents an expanded view of the rising portions of both signals. As can be seen in this figure, the voltage (fast wave) reaches a peak value of 34 V at 1.55 μs (black point). The decay time (full width at half maximum) of the voltage wave is 2.45 μs (blue point). The current reaches a maximum value of 1.8 A, 2.5 μs after the peak of the maximum voltage.
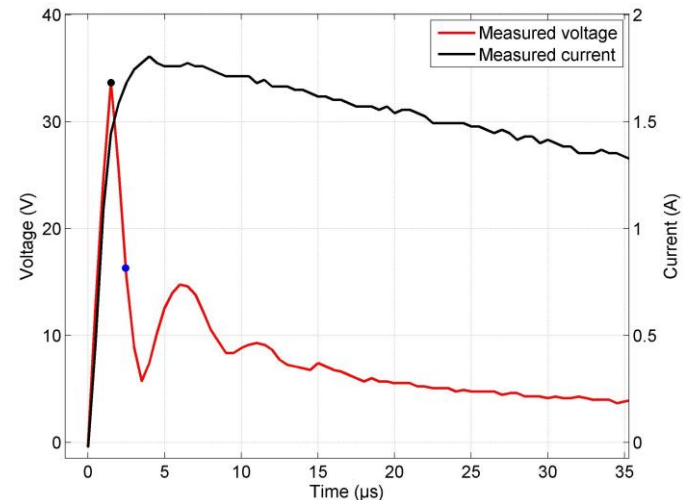

Fig. 5. Expanded view of the rising portions of the measured voltage and current injected into the wind turbine foundation (foundation only).

In a general manner, a signal time response $y(t)$ observed in scattered electromagnetic energy can be represented by the sum of the signal $x(t)$ and the noise present in the system $n(t)$ in accordance with (1),

$$y(t)=x(t)+n(t)=\sum_{n-1}^{M} R_i \cdot \exp(s_i t)+n(t); \quad 0 \le 1 \le T \qquad (1)$$

where: R_i = residues; $s_i = -\alpha_i + j\omega_i$; α_i = damping factors and ω_i = angular frequencies $\omega_i = 2\pi f_i$.

The goal is to find out the best estimation of M, R_i and s_i from the data in a noisy environment. Usually, the simultaneous estimation of these parameters is a nonlinear problem. However, a linearization solution should provide an accurate approach and in some cases the solution is equivalent to solving the original nonlinear problem. In this context, the Matrix Pencil Method (MPM) stands out and was used for the treatment of the measured voltages and currents [9]. To clarify, Fig. 6 shows the original measured voltage and the reconstructed signal using MPM considering 50 poles. Fig. 7 presents an expanded view of the early time of the mentioned signals. The same procedure was adopted for all the measured currents and voltages.
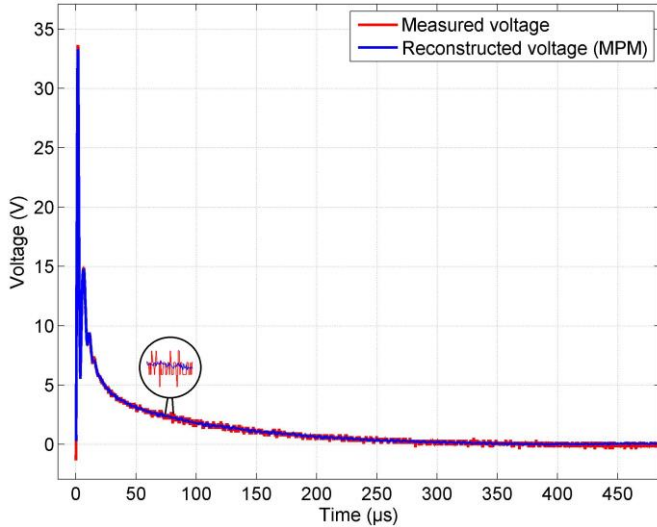

Fig. 6. Measured and reconstructed voltages on the turbine foundation (foundation only).
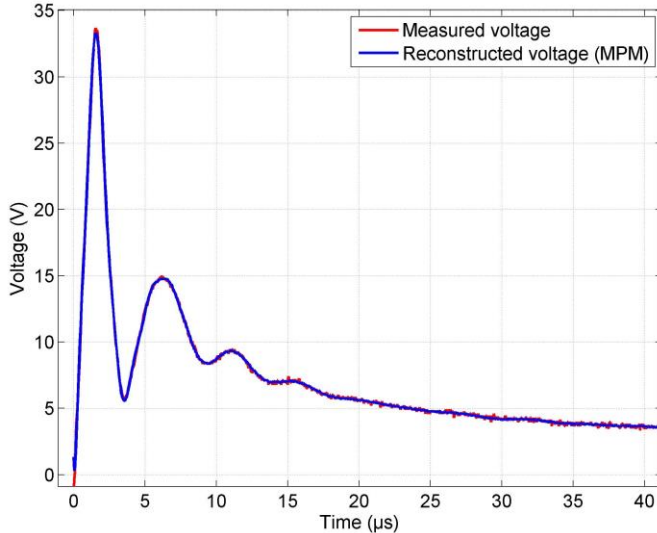

Fig. 7. Expanded view of the measured and reconstructed voltages on the turbine foundation (foundation only).

Considering now the processed signals, the WT grounding impedance can be evaluated in the time domain (TD) and in the frequency domain (FD).

In a TD analysis, the response of a linear circuit subjected to an arbitrary impulse can be calculated using Duhamel's Integral Equation [4]. A discrete solution of $Z(t)$ can be calculated when $V(t)$ and $I(t)$ are obtained experimentally.

Fig. 8 presents the resulting transient grounding impedance in the TD based on the discrete solution of the Duhamel Integral Equation.
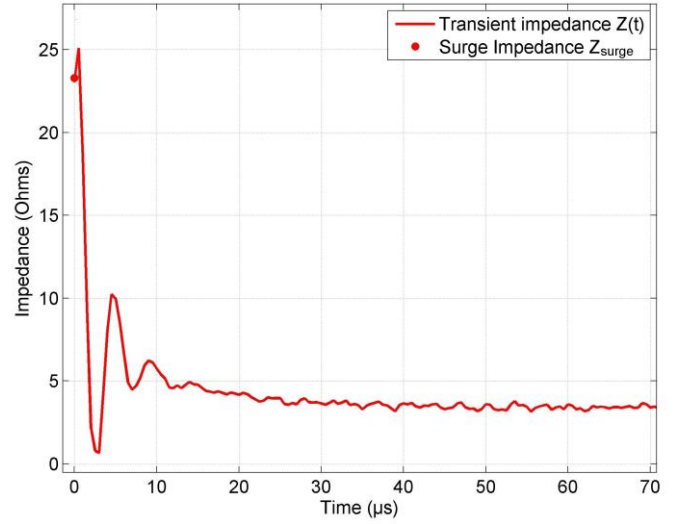

Fig. 8. Transient impedance in the TD of the turbine foundation (foundation only).

By evaluating the transient impedance curve, two important quantities can be observed:
- The surge impedance Z_{surge}, which is defined as the ratio $V(t)/I(t)$ at the moment when $V(t)$ reaches its maximum value [10].
- The static resistance, valid for low frequencies, is the value of the resistance that the impedance curve converges to after the transient period or the steady state impedance value.

Analyzing Fig. 8, the theoretical surge impedance Z_{surge} (red point) can be observed at $t=0+$, which presents a magnitude equal to 23.3 Ω, very close to the maximum impedance value 25.1 Ω. Approximately after 30 μs, the impedance reaches its steady state and the static resistance converges to 4 Ω.

One of the MPM advantages is that once the poles are obtained, the input impedance in the FD, $Z(j\omega)$, can be estimated based on an analytical solution of the Fourier transformation, as can be seen in Fig. 9.

By evaluating the input impedance in the FD, the resistive behavior in the low frequency range up to about 3 kHz, where the impedance is independent of the frequency, can be observed. In this range of frequencies, the input impedance $Z(j\omega)$ approximately assumes the value of the static resistance R. However, for the frequency range above 3 kHz, the inductive behavior is predominant and the impedance is frequency dependent [11].
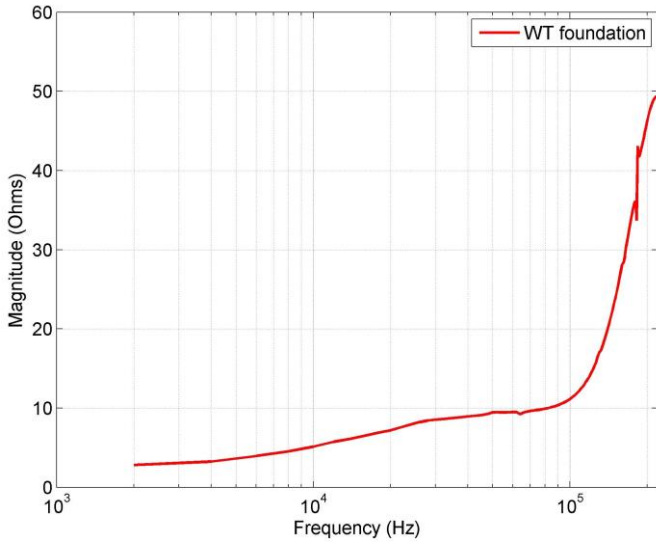
Fig. 9. Input impedance in the FD of the turbine foundation (foundation only).

D. Measurements of the foundation, tower and blades

The same procedure presented previously was adopted in the case of the complete wind turbine, which is composed of the grounding embedded in the foundation, the tower, the nacelle and the blades. The experiment setup was identical to the previous one.

In Fig. 10, the first 40 µs of the transitory period can be observed. For the measurements considering the complete WT, the voltage reaches a peak value of 23 V at 1.65 µs. Its decay time is 2.6 µs. The maximum value of the current, 1.1 A, is reached 1 µs after the peak of the maximum voltage.
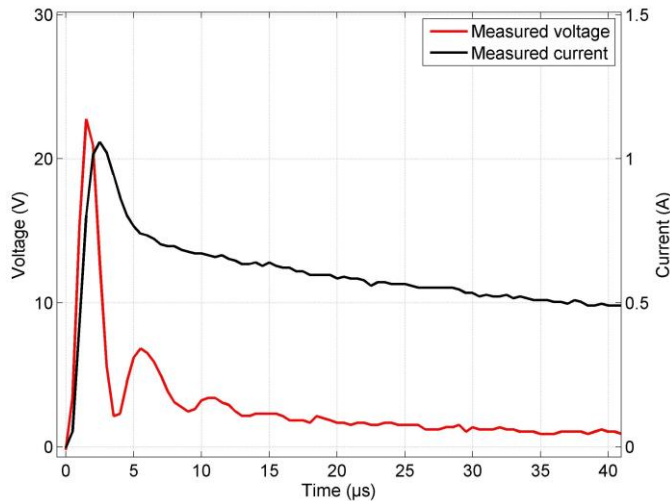

Fig. 10. Expanded view of the rising portions of the measured voltage and current injected into the complete wind turbine (foundation, tower, nacelle and blades).

Fig. 11 presents the evaluation of the Duhamel's Integral (transient impedance curves in the TD) for both scenarios: grounding foundation only and the complete wind turbine.

Based on the transient impedance of the complete wind turbine (blue curve), the theoretical surge impedance Z_{surge} reaches the value of 28.4 Ω, the maximum impedance measured. In the first 10 µs, the transient behavior of the two curves is practically the same. The impedance of the complete

WT reaches its steady state converging to a static resistance R = 2.8 Ω. The small differences between the static resistances (4 Ω to 2.8 Ω) can be attributed to the variation in the soil resistivity in the days when the measurements were carried out. Comparing the results, it can be stated that both scenarios lead to relatively similar behavior in the time domain.
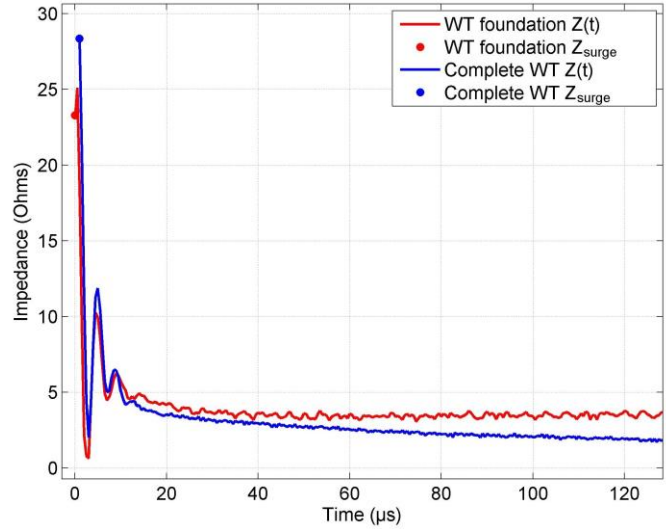

Fig. 11. Transient impedance in the TD of the turbine foundation (foundation only) and for the complete wind turbine (foundation, tower, nacelle and blades).

A frequency domain analysis of the two experiments is presented in Fig. 12. Again, for frequencies above 3 kHz the inductive behavior of high frequencies was observed. The differences observed at low frequencies are again attributed to the variation in the soil electrical parameters in the days when the measurements were carried out. At higher frequencies (beyond about 150 kHz or so), the presence of the complete wind turbine results in an underestimation of the grounding impedance. This is because at these frequencies, the wind turbine (tower, nacelle and blades) presents a finite equivalent impedance in parallel with that of the grounding system, resulting in an overall reduction of the inferred impedance.
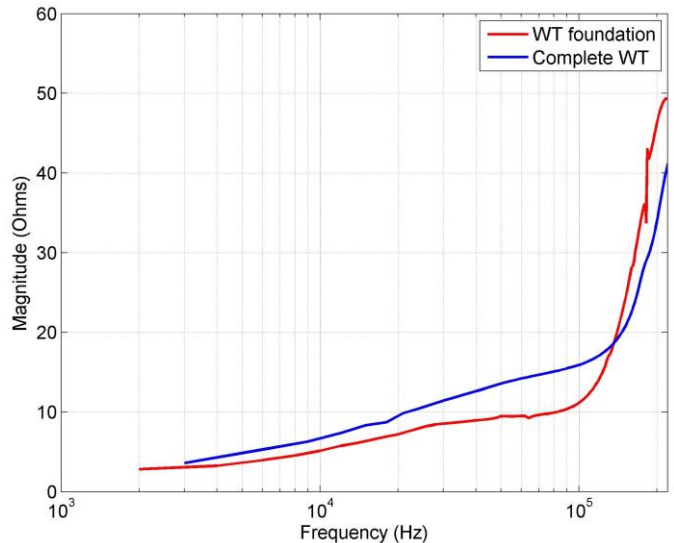

Fig. 12. Input impedance in the FD of the turbine foundation (foundation only) and for the complete WT (foundation, tower, nacelle and blades).

Table II compares quantitatively the results presented in Fig. 12. It can be seen that the differences (Diff.) between the impedance of the foundation only (Found.) and the impedance of the complete structure (C. WT) are appreciable but not significant for the analyzed frequencies. It is expected that at higher frequencies (corresponding to faster injected pulses), the presence of the complete wind turbine would affect the behavior of the impedance in a more significant way.

TABLE II
EVALUATED IMPEDANCES FOR DIFFERENT FREQUENCIES

Z (Ω)	Frequency kHz					
	2	3	4	5	10	20
Found.	2.81	3.02	3.23	3.59	5.13	7.18
C. WT	3.08	3.59	4.16	4.72	6.64	9.46
Diff.	0.27	0.57	0.93	1.13	1.51	2.28
Z (Ω)	Frequency kHz					
	30	40	50	100	200	-
Found.	8.53	8.94	9.46	11.35	46.19	-
C. WT	11.42	12.59	13.54	15.89	33.90	-
Diff.	2.89	3.65	4.08	4.54	-12.19	-

IV. NUMERICAL SIMULATIONS

With the objective to establish representative models suitable for the study of the grounding impedance of tall wind turbines, numerical simulations were carried out. A preliminary study in steady state, in order to determine the low frequency resistance was performed.

Considering the complexity of the entire system composed of the main grounding and numerous conductors and steel reinforced bars present in the foundation of the WT, only the main grounding system was considered in the simulations. Fig. 13 illustrates the implemented configuration.
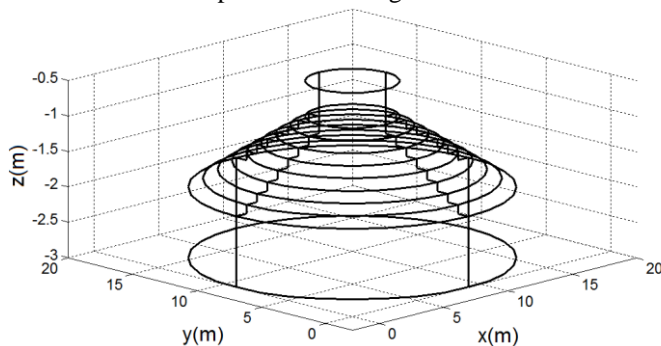

Fig. 13. WT grounding system configuration considered in the simulations.

The steady state study is based on the implementation of the Average Potential Method [12]-[13]. The method divides the grounding electrode into several segments, which have a specific current value. The average electric potential on each segment is computed and matched to the same value of constant electric potential to determine the leakage currents flowing in each segment to the ground. In the implemented procedure, the Method of Images was taken into account making the normal component of the electric field equal to zero in the boundary surface between soil and air.

Considering then the *in situ* soil as a stratified ground with two horizontal layers with the characteristics presented in Section III.B, the grounding system illustrated in Fig. 13 presented a static resistance at low frequencies of 5.9 Ω. This value is conservative and it is in reasonable agreement with the results obtained from the measurements, 4 Ω (see Fig. 8).

V. CONCLUSIONS

This paper presented a study focused on the grounding impedance behavior of wind turbines both in the time and the frequency domains based on *in situ* measurements and numerical simulations. The measurements were performed in a WT located in Mont-Crosin wind park (Switzerland) for two scenarios: only the grounding system embedded in the foundation and the complete WT. Numerical simulations to determine the grounding static resistance at low frequencies were carried out.

Based on the analysis of the measured data in the TD, the transient impedance curves for both cases present practically the same behavior. The surge impedance Z_{surge} for the measurement considering the complete WT assumes a value 5.1 Ω higher than the grounding foundation. However, the static resistance of the complete WT showed a decrease of about 1.2 Ω in comparison with the grounding foundation only. Since the measurements of the complete WT were made 3 months after the measurements considering only the WT grounding foundation, the difference in the low-frequency impedance and in the static resistance may be ascribed, at least in part, to the variations in soil resistivity due to different measurement conditions.

Regarding the FD analysis, the resistive behavior of the grounding systems can be observed in both scenarios for frequencies up to 3 kHz, as well as the frequency dependence of the impedance above 3 kHz characterizing its inductive behavior. At higher frequencies (beyond about 150 kHz or so), the presence of the complete wind turbine resulted in an underestimation of the grounding impedance. It is important to mention that this conclusion was obtained based on a set of collected data and that further investigation taking into account a greater number of measurements is ongoing, as well as the evaluation of the response of the grounding systems for frequencies higher than 200 kHz.

The static resistance obtained numerically based on the Average Potential Method, (5.9 Ω) was in relatively good agreement with the measured data (4 Ω).

Future work will also include numerical simulations of the grounding system response using full-wave methods.

VI. ACKNOWLEDGMENT

VII. References

[1] F. Rachidi, M. Rubinstein, and A. Smorgonskiy, "Lightning protection of large wind-turbine blades," in *Wind Energy Conversion Systems*, S. M. Muyeen, Ed. London: Springer, 2012, pp. 227–241.

[2] A. Elmghairbi, M. Ahmeda, N. Harid, H. Griffiths, and A. Haddad, "A technique to increase the effective length of horizontal earth electrodes and its application to a practical earth electrode system," in *Proc. 2011 7th Asia-Pacific International Conference on Lightning (APL)*, 2011, pp. 690–693.

[3] K. Yamamoto, S. Yanagawa, K. Yamabuki, S. Sekioka, and S. Yokoyama, "Analytical surveys of transient and frequency-dependent grounding characteristics of a wind turbine generator system on the basis of field tests," *IEEE Trans. Power Delivery*, vol. 25, no. 4, pp. 3035–3043, 2010.

[4] A. Smorgonskiy, N. Mora, F. Rachidi, M. Rubinstein, K. Sheshyekani, N. Korovkin, "Measurements of transient grounding impedance of a wind turbine at Mont-Crosin wind park", in *Proc. 2015 Asia Pacific International Symposium on Electromagnetic Compatibility*, Taipei, Taiwan, May 26-29.

[5] V. T. Kontargyri, I. F. Gonos, I. A. Stathopulos, "Study on wind farm grounding system," *IEEE Trans. Industry Applications*, vol. 51, no. 6, pp. 4969-4977, 2015.

[6] S. Visacro, G. Rosado, "Response of grounding electrodes to impulsive currents: an experimental evaluation," in *IEEE Trans. on Electromagnetic Compatibility*, vol. 51, no. 1, pp. 161-164, Feb. 2009.

[7] *IEEE Guide for Measuring Earth Resistivity, Ground Impedance, and Earth Surface Potentials of a Grounding System*, IEEE Std 81-2012 (Revision of IEEE Std 81-1983), pp. 1–86, Dec. 2012.

[8] A. Phillips, "Guide for Transmission Line Grounding, A Roadmap for Design, Testing, and Remediation," EPRI Electric Power Research Institute, Dec. 2004.

[9] T.K. Sarkar and O. Pereira, "Using the matrix pencil method to estimate the parameters of a sum of complex exponentials," *IEEE Antennas and Propagation Magazine*, vol. 37, no. 1, pp. 48–55, Feb. 1995.

[10] L. Grcev and F. Rachidi, "On tower impedances for transient analysis," *IEEE Trans. Power Delivery*, vol. 19, no. 3, pp. 1238–1244, Jul. 2004.

[11] L. Grcev, "Impulse efficiency of simple grounding electrode arrangements," in *Proc. 2007 18th International Zurich Symposium on Electromagnetic Compatibility*, Munich, Germany, Set 24-28.

[12] R. J. Heppe, "Step potentials and body currents near grounds in two layer earths," *IEEE Trans. Power Apparatus and Systems,* vol. 98, no. 1, pp. 45-59, Jan/Feb. 1979.

[13] R. J. Heppe, "Computation of potential at surface above and energized grid or other electrode, allowing for nonuniform current distribution," *IEEE Trans. Power Apparatus and Systems,* vol. 98, no. 6, pp. 1978-1989, Nov. 1979.